Robotics and Autonomous Systems 8 (1991) 239–250
North-Holland

Redundancy resolution for the human-arm-like manipulator

Stefano Chiaverini and Bruno Siciliano

Dipartimento di Informatica e Sistemistica, Università degli Studi di Napoli Federico II, Via Claudio 21, 80125 Napoli, Italy

Olav Egeland

Institutt for teknisk kybernetikk, Norges tekniske høgskole, O.S. Bragstads plass 8, 7034 Trondheim, Norway

Abstract

Chiaverini, S., Siciliano, B. and Egeland, O., Redundancy resolution for the human-arm-like manipulator. Robotics and Autonomous Systems, 8 (1991) 239–250.

The human-arm-like manipulator has a seven-degree-of-freedom kinematic structure obtained by adding a roll joint to the shoulder of the PUMA geometry. This mechanism has higher dexterity than conventional six-degree-of-freedom arms, and allows the elimination of the internal singularities at the shoulder and the wrist. The contribution of the present work is to exploit redundancy to accomplish singularity avoidance and possibly recover the original PUMA design. The inverse kinematics problem is solved at the velocity level by means of a closed-loop algorithm in the framework of task space augmentation with task priority. Three case studies demonstrate the effectiveness of the proposed technique.

Keywords: Kinematics; Redundancy; Singularities.

1. Introduction

It is well known that at least six degrees of freedom are required to arbitrarily assign the position and orientation of a rigid body in space. This is why conventional manipulators have six joints, although the region in which full mobility is available at the end-effector (the dexterous workspace) is a subset of the entire manipulator workspace. The addition of a joint in the kinematic structure is expected to allow a more functional design.

Stefano Chiaverini was born in Napoli, Italy, on December 5, 1961. He received the Laurea and the Research Doctorate degrees in Electronic Engineering from the University of Napoli in 1986 and 1990, respectively. Since 1987 he has been working at the Department of Computer and Systems Science where he is currently a Research Associate. From January to June 1989 he was a Visiting Scientist at the Robotic Laboratory of the German Aerospace Research Establishment (DLR) in Oberpfaffenhofen, Germany, under a NATO Research Fellowship. His research interests include Manipulator Inverse Kinematics Techniques, Redundant Manipulator Control, Cooperative Robot Manipulation, Force/Position Control of Manipulators.

Bruno Siciliano was born in Napoli, Italy, on October 27, 1959. He received the Laurea and the Research Doctorate degrees in Electronic Engineering from the University of Napoli in 1982 and 1987, respectively. Since 1983 he has been working at the Department of Computer and Systems Science where he became a Research Associate in 1989. From Fall 1985 to Spring 1986 he was a Visiting Scientist at the G.W. Woodruff School of Mechanical Engineering, Georgia Institute of Technology, Atlanta, under a NATO Research Fellowship. Since 1991 he is Associate Professor of Automatic Control. His research interests include Manipulator Inverse Kinematics Techniques, Redundant Manipulator Control, Cooperative Robot Manipulation, Control of Lightweight Flexible Arms, Output Feedback Control of Two-Time Scale Systems. Dr. Siciliano is a Technical Editor of *IEEE Transactions on Robotics and Automation*.

0921-8890/92/$05.00

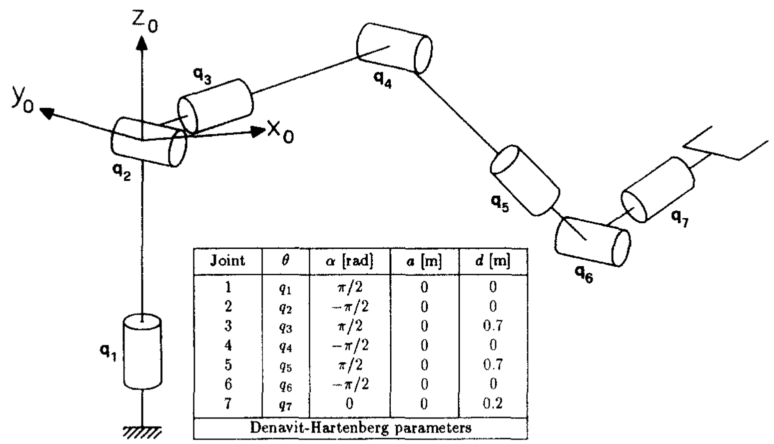

Joint	θ	α [rad]	a [m]	d [m]
1	q_1	$\pi/2$	0	0
2	q_2	$-\pi/2$	0	0
3	q_3	$\pi/2$	0	0.7
4	q_4	$-\pi/2$	0	0
5	q_5	$\pi/2$	0	0.7
6	q_6	$-\pi/2$	0	0
7	q_7	0	0	0.2
Denavit-Hartenberg parameters				

Fig. 1. The seven-joint manipulator

An extra shoulder joint can be added to the widely-adopted PUMA geometry with zero offsets [1]. The resulting manipulator is kinematically redundant, and can reach every point inside its workspace with six degrees of freedom available for end-effector, whereas the original PUMA architecture has wrist and shoulder singularities where the end-effector motion loses degrees of freedom. Not surprisingly, the new geometry is analogous to that of the human arm; namely a spherical shoulder, an elbow, and a spherical wrist. And, indeed, we commonly experience that this seven-joint mechanical arrangement provides us with high manoeuverability in the workspace [2].

Other seven-degree-of-freedom kinematic structures have been studied in the literature, such as the manipulator with a four-degree-of-freedom spherical wrist [3,4], the CYBOTECH robot [5], and the CESAR research manipulator [6]. The evaluation of possible redundant manipulator geometries reported in [7], however, revealed that the human-arm-like design is superior to other designs from the point of view of internal singularities, dexterous workspace, mechanical feasibility, and kinematic simplicity.

The emphasis in the present work is on the avoidance of internal singularities of the considered manipulator, whereas the extra degree of freedom may be useful also for obstacle avoidance and other applications, just like for the dexterous human arm. In particular, we accomplish a kinematic analysis of the structure and evidence mechanical singularities of interest in the shoulder and the wrist.

In order to exploit redundancy, the augmented task space technique is employed [8,9]; we choose a functional constraint task in such a way to avoid the occurence of internal singularities, while possibly keeping the nominal arm configuration as close as possible to the original PUMA design [10]. As a result of this approach, the desirable property of cyclic behaviour [11] may also be obtained, that is closed joint paths are obtained for closed end-effector paths.

The inverse kinematics is then solved at the velocity level by means of the extended Jacobian [12], and the occurrence of artificial singularities

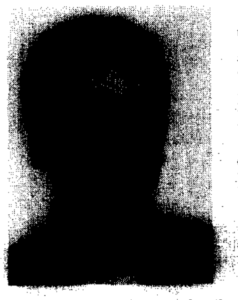

Olav Egeland was born in Trondheim, Norway in 1959. He received the Siv.Ing. and the Dr.Ing. degrees in Electrical Engineering from the Norwegian Institute of Technology in 1984 and 1987, respectively. He became an Assistant Professor at the Norwegian Institute of Technology in 1987, and was at the German Aerospace Research Establishment (DLR) in Oberpfaffenhofen, Germany, in the academic year 1988/89 as a Visiting Scientist. In 1989 he became Professor in Robotics at the Division of Engineering Cybernetics, Norwegian Institute of Technology. His research interests include Kinematics, Dynamics and Control of Manipulators, Kinematically Redundant Manipulators, and Sensory Feedback Control of Robots.

– due to conflicting task situations – is prevented by resorting to the task priority strategy [13,14]. The resulting algorithm is derived in a closed-loop fashion [15] so as to eliminate typical numerical drifts of open-loop techniques. It should be mentioned that preliminary work on this topic is reported in [16].

Finally, we test the performance of the proposed redundancy resolution scheme in three case studies; the first one is aimed at showing the PUMA design recovery capability together with the repeatability of joint trajectories, while the other two evidence the potential of the constrained manipulator to avoid the occurrence of internal singularities.

2. Kinematic analysis

The seven-joint manipulator investigated in this paper mimicks the kinematic structure of the human arm [2]. The manipulator is shown in *Fig. 1*, together with its Denavit-Hartenberg parameters. It is a PUMA-like manipulator with an extra roll joint in the shoulder, which is Joint 3 in *Fig. 1*. As shown in [7], this design is superior to all other possible designs that can be obtained via the addition of a revolute joint to a PUMA manipulator with zero offsets; the criteria that lead to assert the above statement were elimination of internal singularities, optimization of workspace, kinematic simplicity, and mechanical constructability.

Let $\boldsymbol{q}$ denote the 7-dimensional joint vector; thus, the manipulator is kinematically redundant with respect to the 6-dimensional end-effector location vector formally denoted by $\boldsymbol{x}_E$. The first three components of $\boldsymbol{x}_E$ represent the end-effector position vector $\boldsymbol{p}$, while the last three components constitute a three-parameter description for end-effector orientation; such a description has either discontinuities or representation singularities. Therefore, we will use the 3×3 rotation matrix $\boldsymbol{R} = [\boldsymbol{n}\ \boldsymbol{s}\ \boldsymbol{a}]$ from end-effector frame to base frame to represent orientation.

The differential kinematics is described by

$$\boldsymbol{v}_E = \boldsymbol{J}_E(\boldsymbol{q})\dot{\boldsymbol{q}}, \tag{1}$$

where $\boldsymbol{v}_E = [\dot{\boldsymbol{p}}^T\ \boldsymbol{\omega}^T]^T$ is the 6-dimensional end-effector velocity vector, with $\dot{\boldsymbol{p}}$ denoting the 3-dimensional translational velocity vector and $\boldsymbol{\omega}$ the 3-dimensional angular velocity vector; the 6×7 matrix $\boldsymbol{J}_E$ is the end-effector Jacobian that can be computed via geometrical analysis.

In configurations where the Jacobian $\boldsymbol{J}_E$ has full rank, the end-effector has six degrees of freedom. When the Jacobian is rank deficient so that rank $(\boldsymbol{J}_E) = r$, $r < 6$, the end-effector has only r degrees of freedom and the manipulator is said to be in a singular configuration. The dimension of the null space of the Jacobian can be used to find singular points; if it is greater than one, indeed, the manipulator is singular. For the human-arm-like manipulator considered in this work, however, it is quite difficult to derive mechanical singularities in symbolic form. Therefore, a direct analysis based on purely kinematic reasoning may be advisable.

We recall that the PUMA geometry is singular when the second wrist angle is zero, when the wrist point is on the rotational axis of Joint 1, and when the elbow is stretched out [17]. It can be easily proved that both shoulder and wrist singularities are avoided with the new design. Indeed, if the wrist is above the shoulder, it is now possible to move the wrist perpendicular to the major plane of motion; if the wrist is straight, the loss of rotary motion direction is compensated by the new joint [1]. This does not rule out, however, the occurrence of rank deficiencies in the Jacobian matrix corresponding to internal singularities.

Singularities of the human-arm-like manipulator can be found by analyzing the mechanism consisting of Joints 1, 2, and 4–7 while treating Joint 3 as the extra joint, and then the mechanism consisting of Joints 2–7 with Joint 1 as the extra joint. The end-effector will always have six degrees of freedom if either of the two six-joint mechanisms are non-singular. Possible singularities for the manipulator are configurations where both six-joint mechanisms are singular and the extra joint does not provide the degenerate motion.

Joints 1, 2 and 4–7 have the same singularities as the PUMA when $q_3 = 0$, and for a non-zero q_3 it has the elbow singularity $q_2 = 0$, and the wrist singularity $q_6 = 0$. Joints 2–7 are singular if the wrist is singular, the elbow is stretched out or if $q_3 = \pm\pi/2$. This means that the manipulator can only be singular if the wrist is singular or the elbow is stretched out. The elbow singularity occurs on the boundary of the workspace and can-

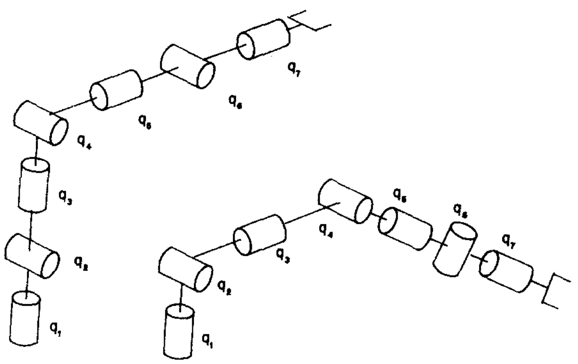

Fig. 2. Singular configurations

not be avoided, se we restrict our attention to the wrist singularity.

The following internal singularities have been identified for the human-arm-like manipulator:
- If $q_6 = 0$ and $q_2 = 0$, there is one null space motion in the wrist and one in the shoulder. This means that the end-effector has at most five degrees of freedom and the manipulator is singular. This singularity was found also in [1].
- If $q_6 = 0$ and $q_5 = \pm\pi/2$, the mechanism consisting of Joints 1, 2 and 4–7 will be singular, and the extra joint 3 will only give a rotation in the plane defined by Joints 5 and 6. The mechanism 2–7 will also be singular, and the motion of the extra Joint 1 will either be in the plane defined by Joints 5 and 6 which happens when $q_3 = 0$, or it will depend on the motion of Joints 2 and 4 to give the required translations in the end-effector. This means that the manipulator is singular.

These singular configurations are shown in *Fig. 2.* [1]

3. Redundancy resolution

Several techniques have been employed in the literature to solve redundancy; see [19,20] for recent surveys.

For the arm at issue, the approach followed in [2] was quite heuristic since it proposed to lock one joint at time, depending on the kind of desired end-effector motion, and then solve the various six-degree-of-freedom mechanisms that were obtained. On the other hand, in [1] redundancy was solved by specifying the self-motion angle about the shoulder/wrist line; however, this accomplishes only avoidance of the first type of singularity. In this respect, it can be said that both techniques were conceptually equivalent to finding an inverse kinematic function for the redundant manipulator [21]; one shortcoming of this method is the difficulty of specifying an explicit function of the joint variables – 'squaring' the inverse kinematics problem – which is valid for any assigned end-effector path. Therefore, it would be nice to generate self-motions in an 'automatic' way, accounting for multiple task specifications.

The PUMA geometry is generally accepted to be a good kinematic structure, so we wish the nominal configuration of the manipulator to be like the PUMA [10]. This is achieved by keeping q_3 close to zero. On the other hand, the main goal of redundancy resolution is to keep the manipulator away from the singular configurations characterized by $(q_2 = 0 \wedge q_6 = 0) \vee (q_5 = \pm\pi/2 \wedge q_6 = 0)$.

Redundancy can be solved at the velocity level; more specifically, Eq. (1) can be inverted to find a joint velocity solution as the sum of the minimum-norm solution and a term in the null space of the Jacobian, i.e. [22]

$$\dot{q} = J_E^{\dagger}(q) v_E + \left[I - J_E^{\dagger}(q) J_E(q) \right] \dot{q}_0, \tag{2}$$

where $J_E^{\dagger}$ is the 7×6 pseudo-inverse of J_E and $\dot{q}_0$ is an arbitrary 7-dimensional joint velocity vector. It can be easily recognized that the term $[I - J_E^{\dagger} J_E]\dot{q}_0$ produces a self-motion of the structure, and then can be conveniently exploited to solve redundancy with no contribution to the end-effector motion.

In the framework of a task space augmentation approach [8,9], redundancy is resolved by imposing a functional constraint task of the joint variables. Since the null space of the Jacobian is 1-dimensional in non-singular configurations, a scalar constraint is considered. Furthermore, this approach has the nice property that, if the end-effector path lies in a simply connected region of the manipulator workspace, the inverse velocity tranformation guarantees cyclic behaviour [11]. This means that a closed path in end-effector

[1] After submission of this paper, a paper appeared [18] which showed that another internal singularity exists for the human-arm-like manipulator; namely, $q_2 = 0$ and $q_3 = \pm\pi/2$. It can be noticed that this singularity is conceptually equivalent to the second singularity described above, by virtue of the symmetry of the structure with respect to the elbow joint.

coordinates will procedure a closed-path in joint coordinates; this is highly desirable in most practical robot applications.

The desired performance is pursued by suitably specifying the constraint to be a function of q_2, q_3, q_5 and q_6. We have chosen

$$x_C = \tfrac{1}{2}(|\sin(q_2)| + 2|\sin(q_6)| + |\cos(q_5)|) + \beta|\cos(q_3)| \tag{3}$$

to the purpose of keeping the manipulator away from singularities, and at the same time preserving the PUMA geometry. The scalar β fixes the relative weight of the above two objectives.

A 7-dimensional constraint Jacobian row vector can be derived as $j_C^T(\boldsymbol{q}) = \partial x_C/\partial \boldsymbol{q}$. At this point, one might be tempted to derive an extended 7×7 Jacobian matrix by adding the above row to the 6×7 end-effector Jacobian in (1), and then solve the squared differential kinematics for the joint velocities. As demonstrated in [10], however, artificial singularities – configurations at which rank deficiencies of the extended Jacobian occur – may arise due to conflicts between the constraint task and the original end-effector task.

The above drawback is overcome by the adoption of the task priority strategy, proposed in [13] and further developed in [14], which prevents the lower priority (constraint) task to interfere with the higher priority (end-effector) task. This is in turn accomplished by projecting the constraint Jacobian onto the null space of the end-effector Jacobian, leading to a joint velocity solution formally equivalent to (2); in this way, the motion of the structure to perform the constraint task is only a self-motion that does not disturb the end-effector motion.

Nonetheless, in order to find the joint variables $\boldsymbol{q}$, solution (2) should be integrated over time; this is inherently an open-loop procedure and then unavoidably suffers from numerical drifts. These can be avoided by the adoption of a closed-loop strategy which accounts for the 'control' deviations.

Regarding the end-effector task, let $\boldsymbol{p}_d$ specify the desired end-effector position vector and $\boldsymbol{R}_d = [\boldsymbol{n}_d \; \boldsymbol{s}_d \; \boldsymbol{a}_d]$ the desired end-effector orientation matrix. The control deviation between desired and actual end-effector location can be expressed as

$$\delta \boldsymbol{x}_E = \begin{bmatrix} \boldsymbol{p}_d - \boldsymbol{p} \\ \delta\boldsymbol{\theta} \end{bmatrix}, \tag{4}$$

where, in particular, $\delta\boldsymbol{\theta}$ is the 3-dimensional vector of angular deviation which is involved in

$$\boldsymbol{R}_d = (\boldsymbol{I} + [\delta\boldsymbol{\theta} \times])\boldsymbol{R}, \tag{5}$$

being $[\delta\boldsymbol{\theta} \times]$ the skew-symmetric form of $\delta\boldsymbol{\theta}$. It can be shown that $\delta\boldsymbol{\theta}$ can be computed as [23]

$$\delta\boldsymbol{\theta} = \tfrac{1}{2}(\boldsymbol{n} \times \boldsymbol{n}_d + \boldsymbol{s} \times \boldsymbol{s}_d + \boldsymbol{a} \times \boldsymbol{a}_d). \tag{6}$$

In order to account for the control deviation, the vector $\boldsymbol{v}_E$ in (2) is modified into

$$\boldsymbol{v}_E = \boldsymbol{v}_{Ed} + \boldsymbol{K}_E \delta\boldsymbol{x}_E, \tag{7}$$

where $\boldsymbol{v}_{Ed}$ is the desired end-effector velocity vector and $\boldsymbol{K}_E$ is a suitable positive definite (diagonal) feedback matrix. This choice implies that

$$\delta\dot{\boldsymbol{x}}_E = -\boldsymbol{K}_E \delta\boldsymbol{x}_E, \tag{8}$$

thus guaranteeing exponential convergence of the end-effector deviation.

On the other hand, for the constraint task the control deviation can be simply chosen as

$$\delta x_C = x_{Cd} - x_C, \tag{9}$$

where x_{Cd} is the desired value of the constraint. Since this value can be typically set to be a constant (in our case the maximum value $2 + \beta$), it is not necessary to compute the pseudoinverse of the constraint Jacobian (projected onto the end-effector Jacobian null space) as in [13,14], but it is sufficient – and computationally advantageous – to use the transpose thereof [24,25]. More specifically, we select the vector $\dot{\boldsymbol{q}}_0$ in (2) as

$$\dot{\boldsymbol{q}}_0 = j_C(\boldsymbol{q}) k_C \delta x_C, \tag{10}$$

where k_C is a positive scalar. This implies that the equation governing the constraint task is

$$\delta\dot{x}_C = -j_C^T(\boldsymbol{q})\boldsymbol{J}_E^\dagger(\boldsymbol{q})\boldsymbol{v}_E - j_C^T(\boldsymbol{q})\left[\boldsymbol{I} - \boldsymbol{J}_E^\dagger(\boldsymbol{q})\boldsymbol{J}_E(\boldsymbol{q})\right] j_C(\boldsymbol{q}) k_C \delta x_C. \tag{11}$$

It can be recognized that the second term on the right-hand side is always negative except when the vector $(\boldsymbol{I} - \boldsymbol{J}_E^\dagger \boldsymbol{J}_E) j_C$ vanishes; but this case corresponds to an artificial singularity where the constraint task cannot be satisfied, given the end-effector task [24]. Therefore, as lons as this case does not occur, we have the result that, by suitably increasing k_C, the constraint control deviation is ultimately bounded along the end-effector path ($\boldsymbol{v}_E \neq 0$), and exponentially tends to zero at steady-state ($\boldsymbol{v}_E = 0$).

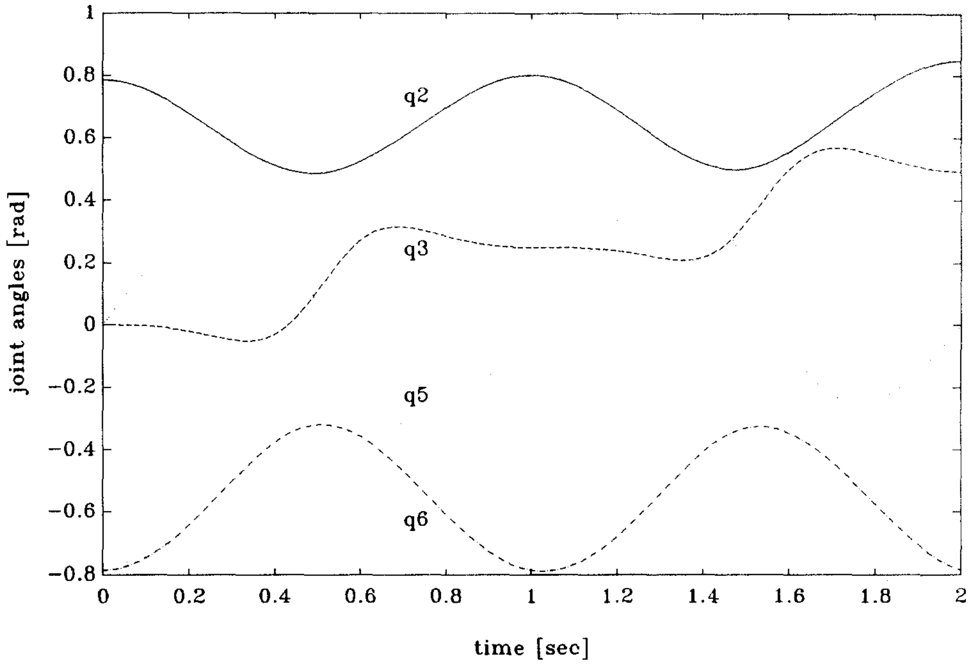

Fig. 3. Joint angles without constraint for Case 1.

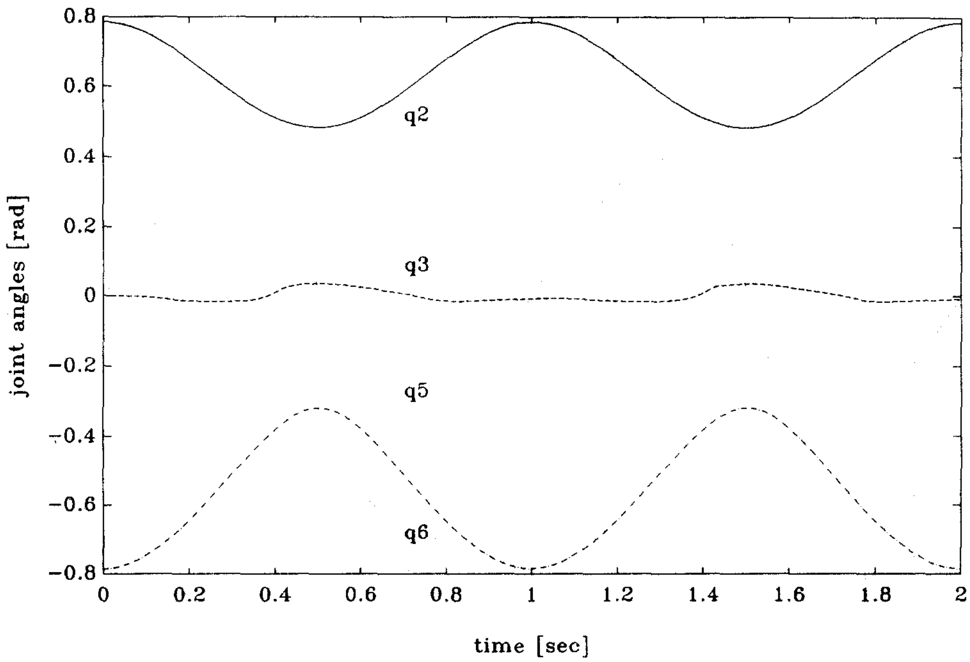

Fig. 4. Joint angles with constraint for Case 1.

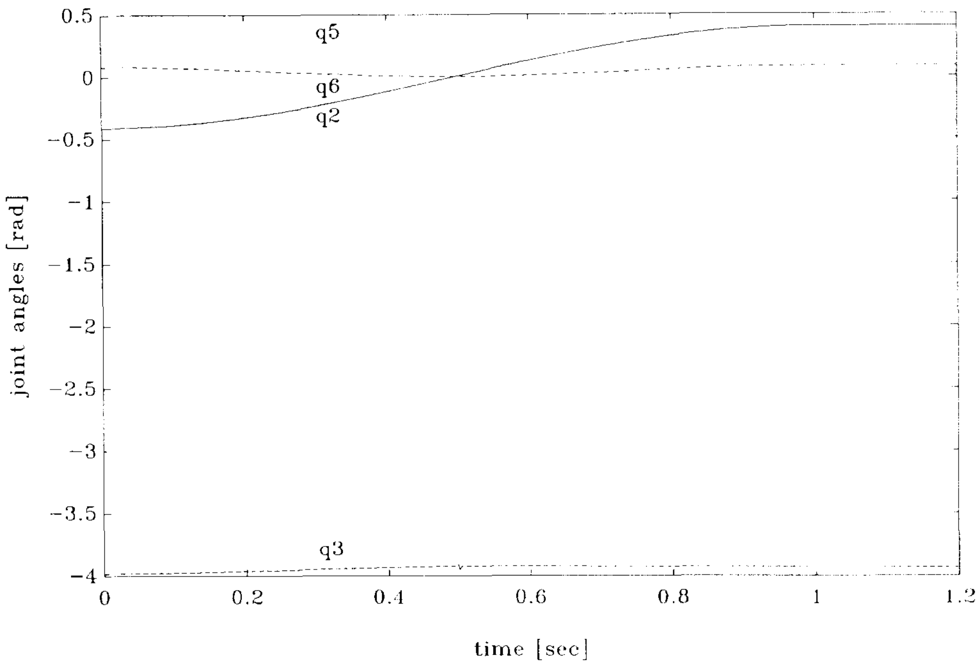

Fig. 5. Joint angles without constraint for Case 2.

4. Case studies

Three case studies have been developed to test the performance of the proposed redundancy resolution scheme for the human-arm-like manipulator.

A discrete version of the algorithm was implemented with Euler integration rule at 2 msec, in view of an on-line implementation of the scheme. We used the software package MATLAB that features the computation of the pseudoinverse of a matrix via its singular value decomposition. The desired end-effector orientation was held constant in all case studies. [2] We chose the feedback gain matrix in (7) as $\boldsymbol{K}_E = 200\ \boldsymbol{I}$, and the feedback scalar in (10) as $k_C = 50$. The proposed solution algorithm was applied first without constraint ($\dot{\boldsymbol{q}}_0 = 0$), and then with constraint. The time histories of the joint variables involved by the constraint (3) are reported below, respectively in the three case studies. The plots relative to end-effector control deviations are omitted, instead, since they correspond to pure numerical errors of the integration routine.

In the first case study, the manipulator is initially placed at the configuration $(0, \pi/4, 0, \pi/2, 0, -\pi/4, 0)$ rad. The desired end-effector position path is a circle in the plane described by $x = p_1$ with center at $(p_1, p_2, p_3 + 0.2)$ m, where p_i's are the initial end-effector position vector components; the angular velocity is 2π rad/sec over the entire path, and the path duration is 2 sec (i.e. two entire cycles). We selected the weighting factor in (3) as $\beta = 20$ to give privilege to the PUMA design recovery objective ($q_3 = 0$). The results in *Figs. 3* and *4* show that: without constraint, the motion of Joint 3 drifts away; with constraint, q_3 is kept close to zero and the joint paths are repeatable after the first cycle, as anticipated in theory. Incidentally, notice that no internal singularity was encountered along the given end-effector path.

In the remaining two case studies, we assigned reference end-effector trajectories with sinusoidal velocity profile of duration 1 sec. This time, we

[2] Observe that this does not imply that the outer three joint angles do not change!

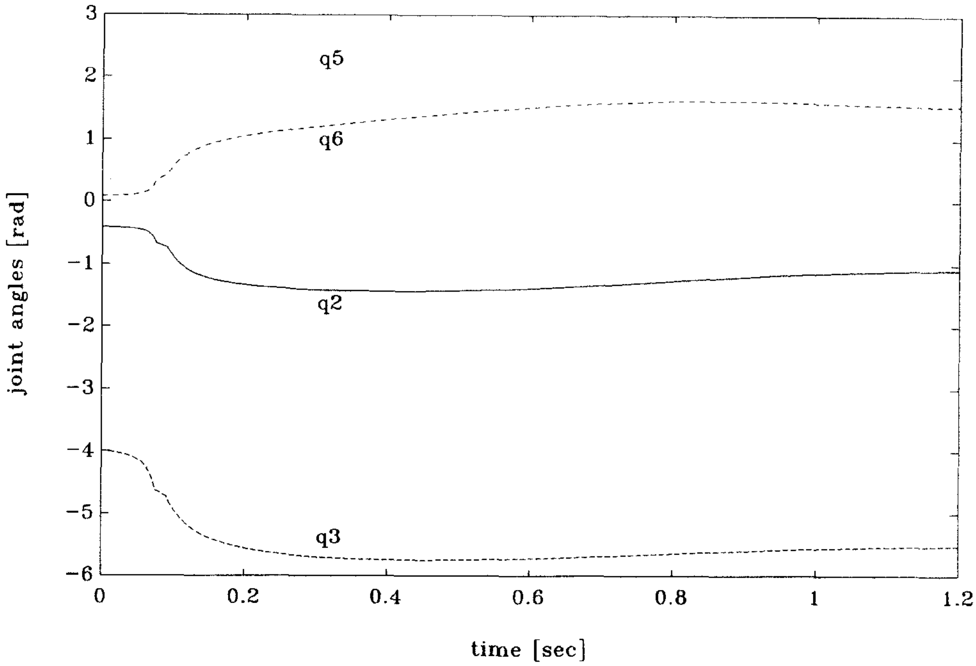

Fig. 6. Joint angles with constraint for Case 2.

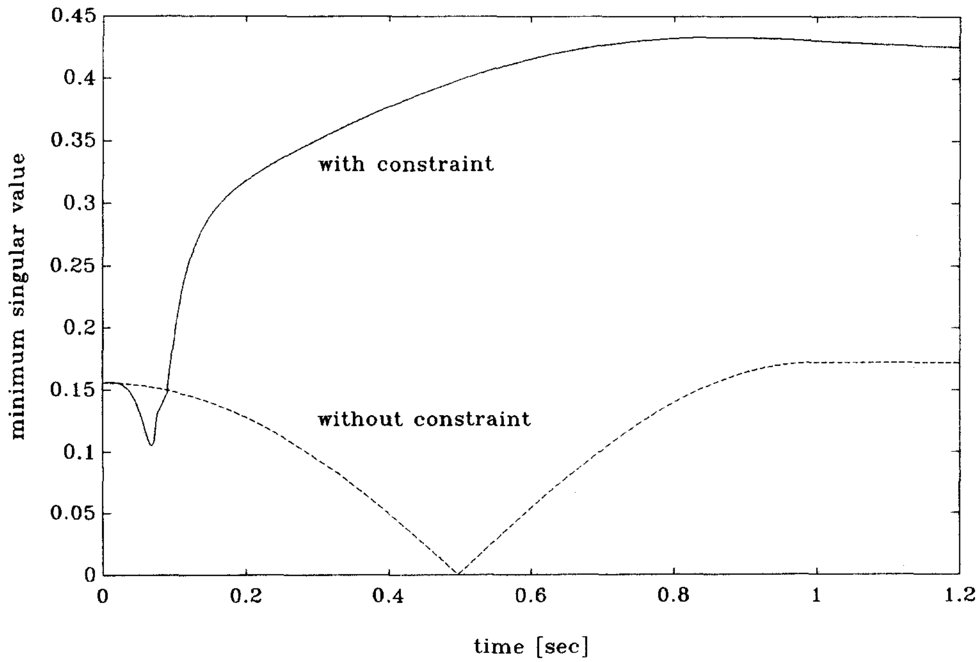

Fig. 7. Minimum singular values for Case 2.

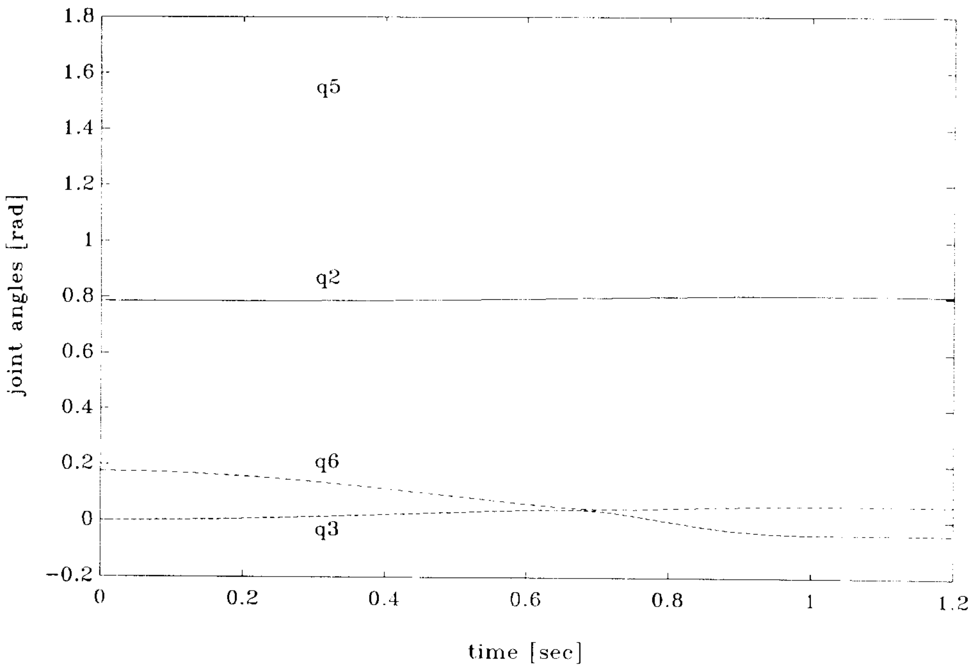

Fig. 8. Joint angles without constraint for Case 3.

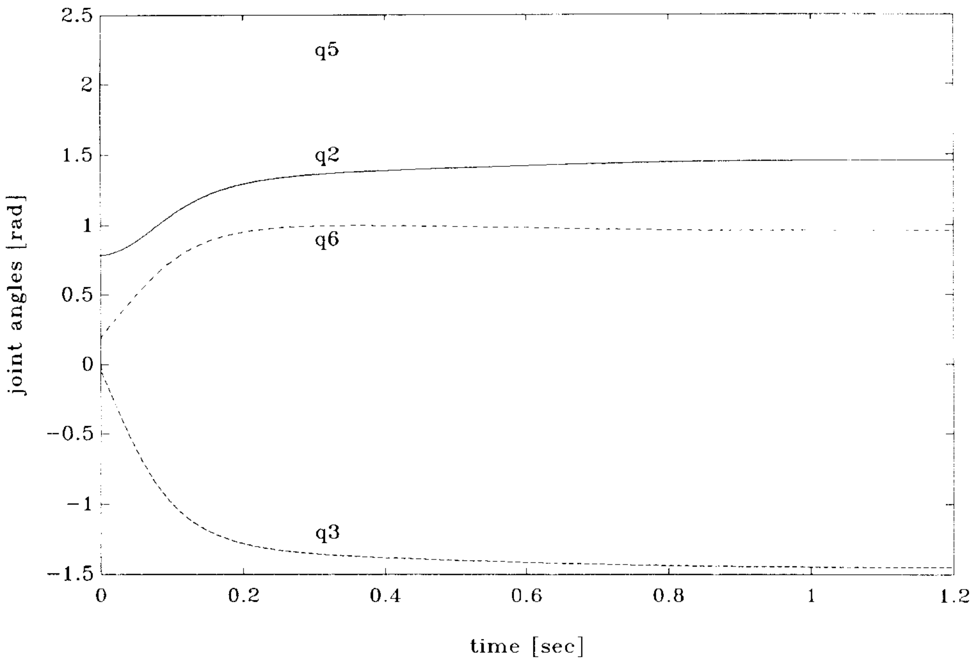

Fig. 9. Joint angles with constraint for Case 3.

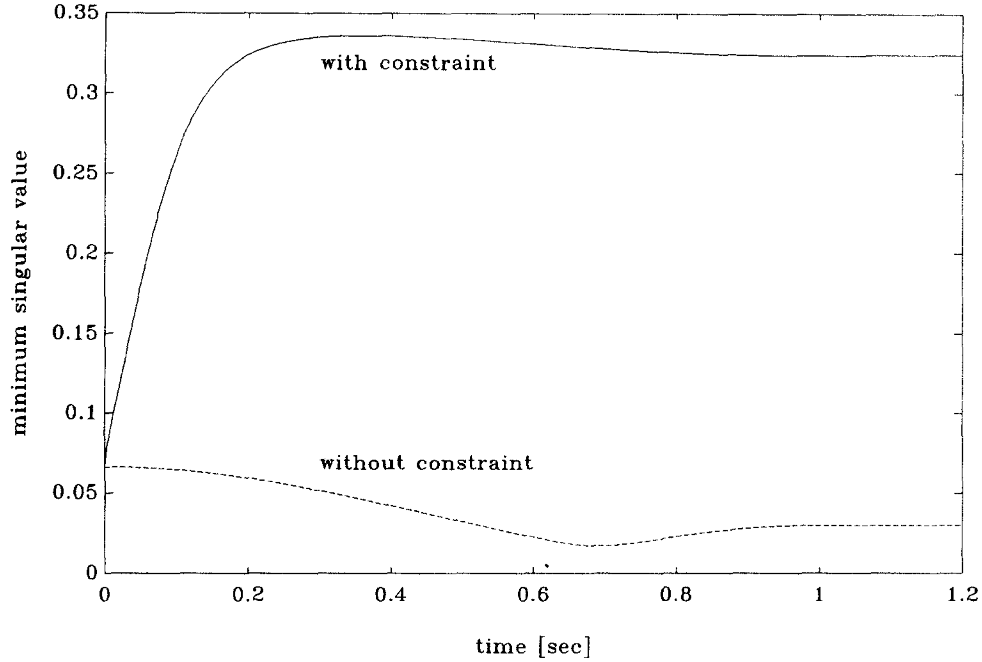

Fig. 10. Minimum singular values for Case 3.

selected the weighting factor in (3) as $\beta = 0.25$ to place much importance on singularity avoidance. The minimum singular value of the end-effector Jacobian matrix is reported over the joint paths to give an accurate estimate of the distance of the manipulator from mechanical singularities [26].

In the second case study, the initial joint configuration is (3.92, -0.413, -3.98, 1.20, 0.273, 0.0842, 0.0318) rad. The desired end-effector position path is a straight line pointing to $(p_1 + 0.4,$ $p_2 + 0.4,$ $p_3)$ m. The results in *Figs. 5* and *7* reveal that, without constraint, the assigned end-effector motion causes the manipulator to fall in the first type of singularity $(q_2 = 0 \wedge q_6 = 0)$. It is interesting to verify that the use of constraint allows the arm to escape the singularity – after a short transient – while executing the given end-effector motion (*Figs. 6* and *7*).

In the third case study, the initial joint configuration is $(0, \pi/4, 0, \pi/2, \pi/2, \pi/18, 0)$ rad. It can be recognized that the arm is close to the second type of singularity $(q_5 = \pm\pi/2 \wedge q_6 = 0)$; this is confirmed by the initial minimum singular value in *Fig. 10*. The desired end-effector position path is a straight line pointing to $(p_1,$ $p_2 - 0.2,$ $p_3)$ m. The results in *Figs. 8* and *10* show that, without constraint, the assigned end-effector motion keeps the arm configuration nearly singular. Instead, with constraint, the manipulator, after a short transient, is driven far from the singularity, attaining more dexterous postures (*Figs. 9* and *10*).

Notice that in the latter two case studies, it was not possible to preserve the PUMA geometry since Joint 3 had to contribute to achieve higher dexterity. This is not a pitfall of the algorithm, as confirmed by the former case study.

5. Conclusions

The human-arm-like manipulator obtained from the PUMA geometry with the addition of a roll joint in the shoulder has been studied in this work. Internal singularities have been found by analyzing the manipulator mechanical structure. An inverse kinematics algorithm based on the augmented task space technique with task priority has been implemented to meet two distinct goals; namely singularity avoidance and PUMA design recovery. Since one single degree of redundancy is available, a scalar functional constraint of the joint variables has been constructed to account for both goals, with a weighting factor between them.

Three significant case studies have demonstrated the possibility of employing the structure with full manipulability inside the workspace by choosing different values of the weighting factor. One open point could be the choice of this factor, since one does now know in advance whether a given end-effector path involves the arm to pass in the neighbourhood of a singular configuration. An answer to this would be to compute the singular value decomposition of the Jacobian matrix on-line, and then tune the factor according to the minimum singular value thereof. Supporting this thesis are the recent results obtained in [27] which show that, due to the particular nature of robotics matrix calculations, the above computation can be feasibly performed – with currently available computer power – for real-time control of manipulators.

Acknowledgements

This work originated from a stay of the authors at DLR, Oberpfaffenhofen, Germany. The financial support of Consiglio Nazionale delle Ricerche under research contract no. 91.01963.PF67, and of Norges Teknisk Naturvitenskapelige Forskningsråd and Norsk Romsenter is gratefully acknowledged.

References

[1] J.M. Hollerbach, Optimum kinematic design for a seven degree of freedom manipulator, in: H. Hanafusa and H. Inoue, eds., *Robotics Research – The Second International Symposium* (MIT Press, Cambridge, MA, 1985) 216–222.

[2] A. Hemami, On a human-arm-like mechanical manipulator, *Robotica* 5 (1987) 23–28.

[3] T. Yoshikawa, Manipulability and redundancy control of robotic mechanisms, *Proc. 1985 IEEE Int. Conf. Robotics and Automation*, St. Louis, MO (1985) 1004–1009.

[4] M.M. Stanišić and G.R. Pennock, A nondegenrate kinematic solution of a seven-jointed robot manipulator, *Int. J. Robotics Research* 4 (2) (1985) 10–20.

[5] F.T. Litvin, V. Parenti Castelli, and M. Shaheen, Singularities in motion and displacement functions for a 7 degree-of-freedom manipulator, *J. Robotic Systems* 4 (1987) 397–421.

[6] R.V. Dubey, J.A. Euler and S.M. Babcock, An efficient gradient projection optimization scheme for a seven-degree-of-freedom redundant robot with spherical wrist, *Proc. 1988 IEEE Int. Conf. Robotics and Automation*, Philadelphia, PA (1988) 28–36.

[7] J.M. Hollerbach, Evaluation of redundant manipulators derived from the PUMA geometry, in: M. Donath and M. Leu, eds., *Proc. ASME Winter Annual Meeting*, Vol 15 (1985) 187–192.

[8] O. Egeland, Task-space tracking with redundant manipulators, *IEEE J. Robotics and Automation* 3 (1987) 471–475.

[9] L. Sciavicco and B. Siciliano, A solution algorithm to the inverse kinematic problem for redundant manipulators, *IEEE J. Robotics and Automation* 4 (1988) 403–410.

[10] O. Egeland, J.R. Sagli, S. Hendseth and F. Wilhelmsen, Dynamic coordination in a manipulator with seven joints, *Proc. 1989 IEEE Int. Conf. Robotics and Automation*, Scottsdale, AZ (1989) 125–130.

[11] D.R. Baker and C.W. Wampler, On the inverse kinematics of redundant manipulators, *Int. J. Robotics Research* 7 (2) (1988) 3–21.

[12] J. Baillieul, Kinematic programming alternatives for redundant manipulators, *Proc. 1985 IEEE Int. Conf. Robotics and Automation*, St. Louis, MO (1985) 722–728.

[13] Y. Nakamura and H. Hanafusa, Task priority based redundancy control of robot manipulators in: H. Hanafusa and H. Inoue, eds., *Robotics Research – The Second International Symposium* (MIT Press, Cambridge, MA, 1985) 155–162.

[14] A.A. Maciejewski and C.A. Klein, Obstacle avoidance for kinematically redundant manipulators in dynamically varying environments, *Int. J. Robotics Research* 4 (3) (1985) 109–117.

[15] L. Sciavicco and B. Siciliano, Coordinate transformation: A solution algorithm for one class of robots, *IEEE Trans. Systems, Man, and Cybernetics* 16 (1986) 550–559.

[16] S. Chiaverini, B. Siciliano and O. Egeland, Kinematic analysis and singularity avoidance for a seven-joint manipulator, *Proc. American Control Conf.*, San Diego, CA (1990) 2300–2305.

[17] R. Featherstone, Position and velocity transformations between robot end-effector coordinates and joint angles, *Int. J. Robotics Research* 2 (2) (1983) 35–45.

[18] K. Kreutz-Delgado, M. Long and H. Seraji, Kinematic analysis of 7 DOF anthropomorphic arms, *Proc. IEEE Int. Conf. Robotics and Automation*, Cincinnati, OH (1990) 824–830.

[19] D.N. Nenchev, Redundancy resolution through local optimazion: A review, *J. Robotic Systems* 6 (1989) 769–798.

[20] B. Siciliano, Kinematic control of redundant robot manipulators: A tutorial, *J. Intelligent and Robotic Systems* 3 (1990) 201–212.

[21] C.W. Wampler, Inverse kinematic functions for redundant manipulators, *Proc. 1987 IEEE Int. Conf. Robotics and Automation*, Raleigh, NC (1987) 610–617.

[22] A. Liégeois, Automatic supervisory control of the config-

uration and behaviour of multibody mechanisms, *IEEE Trans. Systems, Man, and Cybernetics* 7 (1977) 868–871.

[23] J.Y.S. Luh, M.W. Walker and R.P.C. Paul, Resolved acceleration control of mechanical manipulators, *IEEE Trans. Automatic Control* 25 (1980) 468–474.

[24] L. Sciavicco and B. Siciliano, On the solution of inverse kinematics of redundant manipulators, *Prepr. NATO ARW: Robots with Redundancy*, Salò, Italy (1988) (Springer-Verlag) (to be published).

[25] P. Chiacchio and B. Siciliano, A closed-loop Jacobian transpose scheme for solving the inverse kinematics of nonredundant and redundant wrists, *J. Robotic Systems* 6 (1989) 601–630.

[26] C.A. Klein and B.E. Blaho, Dexterity measures for the design and control of kinematically redundant manipulators, *Int. J. Robotics Research* 6 (2) (1987) 72–83.

[27] A.A. Maciejewski and C.A. Klein, The singular value decomposition: Computation and applications to robotics, *Int. J. Robotics Research* 8 (6) (1989) 63–79.